

ADA 040127



2

AD

RDTE Project No. 1-T-0-62111-A-H71

TECOM Project No. 5-CO-403-000-051

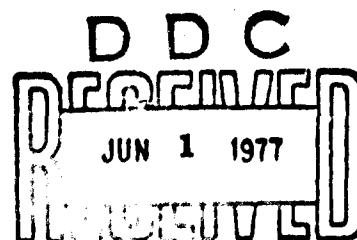
DPG Document No. DPG-TR-M-945A

A STATISTICAL METHOD
OF CALCULATING TURBULENCE
VALUES FOR THE PASQUILL
STABILITY CATEGORIES

TECHNICAL REPORT

MARCH 1977

U.S. ARMY DUGWAY PROVING GROUND
Dugway, Utah 84022



APPROVED FOR PUBLIC RELEASE;
DISTRIBUTION UNLIMITED

AD No. _____
DDC FILE COPY

DISCLAIMER

THE FINDINGS IN THIS DOCUMENT ARE NOT TO BE CONSTRUED AS AN OFFICIAL DEPARTMENT OF THE ARMY POSITION UNLESS SO DESIGNATED BY OTHER AUTHORIZED DOCUMENTS. THE USE OF TRADE NAMES IN THIS REPORT DOES NOT CONSTITUTE AN OFFICIAL ENDORSEMENT OR APPROVAL OF THE USE OF SUCH COMMERCIAL HARDWARE OR SOFTWARE. THIS REPORT MAY NOT BE CITED FOR PURPOSES OF ADVERTISEMENT.

UNCLASSIFIED

SECURITY CLASSIFICATION OF THIS PAGE (When Data Entered)

REPORT DOCUMENTATION PAGE		READ INSTRUCTIONS BEFORE COMPLETING FORM
1. REPORT NUMBER 5-CO-402-000-051	2. JOINT ACCESSION NO.	3. RECIPIENT'S CATALOG NUMBER
4. TITLE (and Subtitle) A STATISTICAL METHOD OF CALCULATING TURBULENCE VALUES FOR THE PASQUILL STABILITY CATEGORIES.		5. TYPE OF REPORT & PERIOD COVERED Technical Report.
7. AUTHOR(s) Albert W. Waldron, Jr.		6. PERFORMING ORG. REPORT NUMBER
9. PERFORMING ORGANIZATION NAME AND ADDRESS U. S. Army Dugway Proving Ground, Dugway, UT 84022		8. CONTRACT OR GRANT NUMBER(s) DPG-TR-M-945A
11. CONTROLLING OFFICE NAME AND ADDRESS U. S. Army Dugway Proving Ground Dugway, UT 84022		10. PROGRAM ELEMENT, PROJECT, TASK AREA & WORK UNIT NUMBERS 1T062111AH71
14. MONITORING AGENCY NAME & ADDRESS (if different from Controlling Office)		12. REPORT DATE 11 1977
		13. NUMBER OF PAGES 29 (12) 38 p.
		15. SECURITY CLASS. (of this report) UNCLASSIFIED
		16a. DECLASSIFICATION/DOWNGRADING SCHEDULE
16. DISTRIBUTION STATEMENT (of this Report) Approved for public release; distribution unlimited.		
17. DISTRIBUTION STATEMENT (of the abstract entered in Block 20, if different from Report)		
18. SUPPLEMENTARY NOTES		
19. KEY WORDS (Continue on reverse side if necessary and identify by block number) Aerosol diffusion categories, bulk Richardson's number, horizontal diffusion, Monin-Obukhov length scale, net radiation, Pasquill stability classes, Richard- son's number, similarity theory, turbulence estimation, Turner diffusion classification system, vertical diffusion		
20. ABSTRACT (Continue on reverse side if necessary and identify by block number) This paper demonstrates the feasibility of estimating vertical and horizon- tal turbulence values from wind speed and vertical temperature gradient. It is shown that daytime solar angle is highly correlated with vertical temperature gradient. Vertical temperature gradient is also correlated with measured net radiation. At night, vertical temperature gradient is correlated with net radiation and wind speed. Bulk Richardson's number can be calculated from vertical temperature gradient and wind speed. Monin-Obukhov length scale		

DD FORM 1 JAN 73 1473

EDITION OF NOV 68 IS OBSOLETE

UNCLASSIFIED

SECURITY CLASSIFICATION OF THIS PAGE (When Data Entered)

COP 118 150

20. ABSTRACT(Continued)

→ can be calculated from bulk Richardson's number.

It is shown from Kansas "Windy Acres" data that horizontal and vertical turbulence can be estimated from surface roughness, Monin-Obukhov length scale and wind speed. Hence turbulence values can be assigned for each vertical temperature gradient, wind speed combination. The associated Pasquill category can be determined from the turbulence values. ↗

TABLE OF CONTENTS

SECTION 1. SUMMARY

	Page
1.1 BACKGROUND	1
1.2 PURPOSE OF STUDY	2
1.3 DESCRIPTION AND SCOPE OF STUDY	2
1.4 SUMMARY OF RESULTS	2
1.5 CONCLUSIONS	2
1.6 RECOMMENDATIONS	3

SECTION 2. DETAILS OF STUDY

2.1 OBJECTIVES	3
2.2 LITERATURE REVIEW	4
2.3 METHOD	7
2.4 CALCULATED RESULTS	8
2.5 ANALYSIS	28
2.6 CONCLUSIONS	28

SECTION 3. APPENDICES

A. REFERENCES	A-1
B. DISTRIBUTION LIST	B-1

BY _____
DISTRIBUTION AVAILABILITY CLASS
OCL ATIC ACTION SPECIAL
A

LIST OF TABLES

<u>Table</u>		<u>Page</u>
1	Diffusion Classification Systems	5
2	Relations Between Pasquill Class, σ_E and σ_A	5
3	Daytime Net Radiation Index and Associated Kansas Vertical Potential Temperature Gradient	10
4	Nighttime Vertical Potential Temperature Gradient by Radiation Index and Wind Speed	10
5	Net Radiation Index	11
6	Comparison of Kansas u_* Values at 5.66 and 22.63 Meters . .	11
7	Dependent Data Results for σ_E , Unstable Case	12
8	Dependent Data Results for σ_E , Stable Case	13
9	Dependent Data Results for σ_A , Unstable Case	14
10	Dependent Data Results for σ_A , Stable Case	14
11	Independent Data Prediction of 15-Minute Turbulence Values at 5.66 m Using Bulk Richardson's Number and Observed Wind Speed	15
12	One-Hour Average σ_E Results for the Unstable Case	15
13	One-Hour Average σ_E Results for the Stable Case	15
14	One-Hour Average σ_A Results for the Unstable Case	16
15	One-Hour Average σ_A Results for the Stable Case	16
16	Standard Error Divided by the Mean Observed Standard Deviation	17
17	Predicted Values of 5.66 m σ_E and σ_A Using Bulk Richardson's Number	17
18	Results of Regression Equations for p, α and β as Functions of $10^5 z_0/L$ and \bar{u}	19
19	Results of Regression Equations for p, α and β as Functions of β and \bar{u}	19

<u>Table</u>		<u>Page</u>
20	Values of L and 1/L by Wind Speed and Radiation Index Class	21
21	Expected 5.66 σ_E and σ_A Values for Each Radiation Index and Wind Speed.	22
22	Power Law Exponents for 5.66 to 22.63 m Gradients of \bar{u} , σ_A and σ_E	22
23	Expected 22.63 m σ_E and σ_A Values for 5.66 m Net Radiation Index and Wind Speed.	23
24	Comparison of 5.66 m σ_E Values Obtained by Three Methods. . .	25
25	Expected 10 m σ_E and σ_A Values for 10 m Wind Speed and 5.66 m Net Radiation Index.	26
26	Pasquill Stability Categories for Kansas Data	27

SECTION 1. REPORT SUMMARY

1.1 BACKGROUND

In many cases, it has been necessary to estimate atmospheric pollution from known sources without adequate measures of turbulence. Several schemes have been formulated to estimate turbulent diffusion. There are fewer schemes for accurately estimating turbulence. To estimate diffusion, Pasquill, in an unpublished note, suggested six stability classes expressed in terms of wind speed and degree of insolation. Gifford⁽¹⁾ prepared graphs of vertical and horizontal cloud growth using Pasquill's ideas. In 1964, Turner⁽²⁾ estimated net radiation from cloud cover, ceiling height, and solar angle. The United States Nuclear Regulatory Commission (NRC)⁽³⁾ categorized stability classes as a function of vertical temperature gradient ($\Delta T/\Delta z$).

Two significant controlling parameters for turbulence in a steady-state surface boundary layer are surface roughness (z_0) and Monin-Obukhov length scale (L). Relatively independent of height, L can be determined from the wind speed and vertical temperature gradients. Panofsky and Prasad⁽⁴⁾ have related vertical turbulence to height (z), z_0 and L . Data from the Great Plains,⁽⁵⁾ Wangara⁽⁶⁾ and Kansas⁽⁷⁾ experiments can be used to clarify the relationships between turbulence and the various profile parameters. Panofsky's L , z_0 and z do not totally define vertical turbulence (σ_E). It can be shown that wind speed (\bar{u}) is a fourth influence. Golder⁽⁸⁾ used $1/L$ and z_0 to define the stability class in the lowest 16 meters, but ignored the additional influence of wind speed. The NRC $\Delta T/\Delta z$ basis of classification ignores the influence of wind speed and stability as defined by Richardson's number (Ri) or L . In short, none of the current classification systems include all the variables which influence turbulence, and most fail to consider the change of this influence with height.

1.2 PURPOSE OF STUDY

The purpose of this study is to demonstrate from Great Plains, Wangara, and Kansas data that a more comprehensive system of turbulence estimation in the surface boundary layer can be devised for an individual site. The classification will not be universal. The required regression equations will be site-dependent. The output will be the σ_E , horizontal turbulence (σ_A) and \bar{u} profiles. The input will be wind speed, net radiation (R), and surface roughness.

1.3 DESCRIPTION AND SCOPE OF STUDY

A simple basis of $\Delta T/\Delta z$ estimation is quantified. Methods of calculating z_0 are demonstrated. Regression equations are formulated for Kansas data to show that the standard deviations of the vertical elevation angle and the horizontal azimuth at 5.66 meters are primarily functions of $\frac{z_0}{L}$ and \bar{u} . Vertical gradients of σ_E and σ_A are functions of the power-law wind-profile exponent (p). In turn, p is a function of $\frac{z_0}{L}$ and \bar{u} .

1.4 SUMMARY OF RESULTS

Regression equations for σ_A and σ_E at 5.66 m developed for Kansas data predict values highly correlated to the observed. σ_A can be adequately predicted for 1 hour but is less predictable for 15 minutes.

1.5 CONCLUSIONS

Vertical and horizontal turbulence can be accurately predicted for the surface boundary layer, from measured values of vertical temperature gradient, surface roughness, horizontal wind speed, and vertical wind speed gradient. Vertical temperature gradient can be estimated from measured net radiation during the day and from net radiation plus wind speed at night. The power-law wind-speed exponent p can be estimated from the derived quantity $\frac{z_0}{L}$ and observed wind speed.

The above would suggest that after the first site evaluation using full instrumentation, that σ_E and σ_A values could be obtained from the resultant regression equations based on wind speed, roughness, and net radiation measurements only. This is contrary to the findings of Luna, (9) who found that only direct measurements of turbulence would suffice. Vertical gradients of σ_E and σ_A are governed by power-law exponents β and α . In turn, β and α are functions of p .

1.6 RECOMMENDATION

Published data from future micrometeorological experiments should include data on cloud cover and height as well as measurements made with an integrating net radiometer. The regression equations resulting from such experiments would indicate possible bases of obtaining more universal dimensionless equations for intensity of turbulence.

SECTION 2. DETAILS OF STUDY

2.1 OBJECTIVES

The objective of this study is to use past data to indicate a method of minimizing the cost of making a continuous collection of turbulence data. Requirements include:

- a. In-depth studies of particular sites to compare measured turbulence parameters with wind and temperature profile data
- b. Determination of a basis of estimating vertical temperature gradient from measured net radiation and wind speed
- c. Demonstration that it is feasible to utilize $\Delta T/\Delta z$ and \bar{u} to calculate:
 - i) σ_E and α_A
 - ii) p
 - iii) α and β

d. Indication that measured net radiation and wind speed at one level can be used to produce estimates of turbulence superior to those resulting from the use of sun's angle, cloudiness, and wind speed during the day; or cloud cover and wind speed at night

2.2 LITERATURE REVIEW

2.2.1 Turbulent Diffusion Typing Methods

a. F.A. Gifford⁽¹⁰⁾ review. In the Gifford review, several typing methods are discussed. Some of these methods are summarized in Table 1.

If one assumes rectilinear expansion from source to 100 meters, values of σ_E and σ_A can be determined for each Pasquill stability category as given in Turner⁽²⁾. These values appear in Table 2.

Prasad⁽¹¹⁾ related Ri to bulk Richardson's number (B). B is a particularly convenient parameter, since at any given height, it depends on vertical potential temperature gradient and wind speed only.

b. Comment.

All of the above systems include cloud-growth rates different from a constant times distance to the power of 1. The choice of stability class, release height and cloud-growth rate are primary considerations. The choice of σ_E and σ_A and their change with height are secondary.

2.2.2 Theory

Similarity theory states that steady state vertical turbulence normalized by friction velocity (u_*) in the surface boundary layer is completely determined by surface roughness, height and Monin Obukhov length scale. The surface boundary layer is the layer of air above the earth's surface in which u_* is constant with height. L can be calculated from Ri. Businger⁽¹²⁾ showed that:

$$Ri = \frac{0.74 \zeta (1 - 15\zeta)^{1/2}}{(1 - 9\zeta)^{1/2}} \quad \text{for } \zeta < 0 \quad (1)$$

Table 1. Diffusion Classification Systems

System	Stability Classes	Indicator
1. Pasquill:	6	Insolation, cloud cover and wind speed
2. Brookhaven National Laboratory	5	$\Delta T/\Delta z$ per 123 meters (m) and 108 m \bar{u}
3. Turner	7	Solar Angle, cloud amount and height, 10 m \bar{u}
4. Golder	6	1/L and z_0 (2-16 meters)
5. Cramer	4	Measured values of σ_E and σ_A
6. TVA	6	$\frac{\Delta \theta^a}{\Delta z}$ $^{\circ}\text{K}/100$ m for 75-250 m
7. Briggs	7	Insolation, cloud cover and wind speed

a. θ = potential temperature in degrees ($^{\circ}$) Kelvin (K)

Table 2. Relations between Pasquill Class, σ_E and σ_A

Turbulence	Pasquill Stability Class					
	A	B	C	D	E	F
σ_E°	> 7.35	5.21-7.35	3.35-5.2	2.31-3.34	1.61-2.3	≤ 1.6
σ_A°	> 13	8.88-13	5.76-8.87	3.98-5.75	2.81-3.97	≤ 2.8

where

$$\zeta = z/L$$

z = height above the ground

$$Ri = \frac{0.74\zeta + 4.7\zeta^2}{(1 + 4.7\zeta)^2} \quad \text{for } \zeta > 0. \quad (2)$$

Richardson's number is obtained from:

$$Ri = \frac{g}{T} \frac{(\partial\theta/\partial z)}{(\partial u/\partial z)^2} \quad (3)$$

where

g = acceleration of gravity, m/second²(s²)

T = absolute temperature, °C

$\partial\theta/\partial z$ = vertical potential temperature gradient, °C/m

$\partial u/\partial z$ = vertical wind speed gradient, s⁻¹

To determine whether a given set of data are steady state, u_* is obtained for different vertical layers from the equations:

$$\frac{\bar{u}}{u_*} = \frac{1}{k} (\ln(z/z_0) - \psi_1(\zeta)) \quad \zeta < 0 \quad (4)$$

$$\text{and} \quad \frac{\bar{u}}{u_*} = \frac{1}{k} (\ln(z/z_0) + 4.7\zeta) \quad \zeta > 0 \quad (5)$$

where k = von Karman's constant = 0.35

$$\psi_1(\zeta) = 2\ln((1+x)/2) + \ln((1+x^2)/2) - 2\tan^{-1}x + \pi/2 \quad (5a)$$

$$x = (1 - 15\zeta)^{1/4}$$

Having satisfied the requirement of constant u_* with height, the next one is to find a satisfactory substitute for Ri, since the vertical wind speed gradient is frequently not available. Bulk Richardson's number is a candidate since it can be calculated from $\partial\theta/\partial z$, \bar{u} , and T:

$$B = \frac{g}{T} \frac{\partial\theta/\partial z}{\bar{u}^2} z^2 \quad (6)$$

where the definitions of the variables are the same as for Equation 3 above.

To relate Ri and B , Prasad⁽¹¹⁾ showed that:

$$Ri = B \left(\frac{\ln(z/z_0) - \psi_1(z)}{\phi(Ri)} \right)^2 \quad (7)$$

where

ψ_1 is the same as in Equation 5a above

$$\phi = (1 - 18Ri)^{-\frac{1}{4}} \quad Ri < 0$$

and

$$\begin{aligned} \psi_1(Ri) &= - \frac{5Ri}{(1 - 5Ri)} \\ \phi(Ri) &= \frac{1}{(1 - 5Ri)} \quad Ri > 0 \end{aligned}$$

The question then arises as to whether the relationships of vertical turbulence, σ_E and horizontal turbulence σ_A to B , z_0 and \bar{u} are as precise as their relationship to L , z_0 and \bar{u} . If they are, adequate estimates of turbulence can be obtained from the vertical potential temperature gradient, wind speed and roughness. The vertical potential temperature gradient can be measured, estimated from net radiation and wind speed, or grossly estimated from solar angle, season and cloud cover. All of these bases of estimating the vertical potential temperature gradient are site-dependent.

2.3 METHOD

2.3.1 General

Great Plains data are used to show a high correlation between insolation (I) measured by a pyrheliometer and net radiation (R) measured by a Gier and Dunkle net radiometer. Wangara data are used to show that during daylight hours, ΔT is highly correlated with R , and at

night it is correlated with R and \bar{u} . Kansas data will be used to show that, given the 5.66 m \bar{u} and the 4-8 m $\Delta T/\Delta z$, that R_i , z/L , σ_E , σ_A , p , α and β are defined in the surface boundary layer from 4 to 32 meters.

2.4 CALCULATED RESULTS

2.4.1 Radiation Measurements. The Great Plains trials⁽⁵⁾ were conducted during the summer of 1953, 5 miles east-northeast of O'Neill, Nebraska. Participants came from the staffs of five universities. Shortwave radiation (I) measured by an Eppley pyrhelimeter was compared to net radiation (R) measured by a Gier and Dunkle net radiometer. The correlation between the two for 58 measurements was 0.92, where:

$$R = 0.644I - 38.74 \quad (8)$$

where

R = net radiation in (mcal)/(cm² min)

I = short wave radiation in mcal cm⁻² min⁻¹

2.4.2 Relationship of Vertical Temperature Gradient to Net Radiation and Wind Speed

Wangara data⁽⁶⁾ included a 40-day collection of wind speed at six levels and vertical temperature gradient from 1 to 2 and 2 to 4 meters. Net radiation was measured by a Funk net radiometer. All micrometeorological data were averaged for a half hour centered on the hour, 24 times per day. The data were collected during the winter of 1967 near Hay, N.S.W., Australia (34°30' S, 144°56' E).

Net radiometer readings at noon and midnight were related to the 2-4 m temperature difference as follows:

$$\text{At noon: } \Delta T = -0.00898R - 0.0023 \quad (9)$$

where

R = net radiation in milliwatts/cm² (mw/cm²)

ΔT = $T(4 \text{ m}) - T(2 \text{ m})$ in degrees centigrade

Number of cases (n) = 35

Correlation coefficient (r) = 0.86

$$\text{At midnight: } \Delta T = -0.0445R - 0.08512\bar{u} + 0.44576 \quad (10)$$

where

\bar{u} = 4 m wind speed in meters per second

Number of cases = 38

$r = 0.61$

The Wangara nighttime vertical temperature gradients were somewhat variable in time, suggesting unsteady conditions. Also, the relationship between the ΔT from 1 to 2 m and that between 2 and 4 m was quite variable. Temperatures at more levels would make it possible to smooth the vertical temperature gradient. This was done for Kansas⁽⁷⁾ data using second-order polynomial equations to fit the vertical profiles.

The cloud coverage was observed at Wangara. For midnight data, the nighttime Pasquill cloud classification of 0.5 or more low or middle clouds was associated with $R \geq -4.0 \text{ mw/cm}^2$ for 73% of the cases. Low or middle cloud cover of less than 0.5 was associated with $R < -4.0 \text{ mw/cm}^2$ 85% of the time. The minimum net radiation at midnight was -8.4 mw/cm^2 .

2.4.3 The Relationship between Vertical Temperature Gradient, Wind Speed, Net Radiation and Stability Class for 1 Hour

The daytime insolation class can be determined as a function of solar angle and cloud cover, as a function of I, or as a function of R. Since the vertical temperature gradient is a function of R and site characteristics, it becomes necessary to determine the temperature gradient category independently for each site. Neither cloud cover nor net radiation statistics are available for the Kansas site; hence, it was necessary to determine the 4 - 8 m potential temperature gradient radiation class empirically as a function of solar angle class. The solar-angle radiation index was determined by Turner⁽¹³⁾. The relationship of solar angle to potential temperature gradient at Kansas is presented in Table 3. The potential temperature gradients used are 1-hour averages.

Table 3. Daytime Net Radiation Index and Associated Kansas Vertical Potential Temperature Gradient

Solar Angle, degrees	Net Radiation Index	$\partial\theta/\partial z$, °C/m
< 15	1	> -0.07
15-35	2	-0.07 to -0.1
35-60	3	-0.101 to -0.115
>60	4	< -0.115

Nighttime vertical temperature gradient is a function of R and \bar{u} . Since there are no published hourly values of R or cloud cover for the Kansas experiment, the first estimate of the vertical potential temperature gradient can be determined from the Wangara equation 10 above, where:

$$\partial\theta/\partial z = \Delta T/\Delta z + 0.01 \text{ } ^\circ\text{C/m}$$

The resulting 4 to 8 meter potential temperature gradients are seen in Table 4.

Table 4. Nighttime Vertical Potential Temperature Gradient by Radiation Index and Wind Speed

\bar{u} , m/s	Net Radiation Index R, mm/cm ²	-1 -4	-2 -8
1		0.137	0.182
2		0.116	0.160
3		0.095	0.139
4		0.073	0.118
5		0.052	0.096
6		0.031	0.075
7		0.010	0.054
8		0.0	0.033
9		0.0	0.011

The values in Table 4 correspond reasonably well to the nighttime 1-hour 4-to-8-meter potential temperature gradients at the Kansas site.

A more complete form of Table 3 comes from Turner⁽¹³⁾. The results are seen in Table 5.

Table 5. Net Radiation Index

	Day					Night**	
	0 - 5	6 - 9			10	0 - 4	5 - 10
Cloud Cover (1/10)		< 7	7 - 16	> 16	< 7	> 7	
Cloud Height (1000 ft)							
Solar Angle: < 15°	1	1	1	1	0	1	-2 -1
15 - 35°	2	1	1	2	0	1	
35 - 60°	3	1	2	3	0	2	
> 60°	4	2	3	4	0	3	

**Nighttime is defined as the period from 1 hour before sunset to 1 hour after sunrise.

2.4.4 The Steady State Requirement

Since there is little in the literature to show the close correspondence between wind speed and temperature profile data and turbulence, it is in order to examine possible relationships using the best data available. The Kansas "Windy Acres" data published by Izumi⁽⁷⁾ meet the qualification. The first requirement for the comparison is that the data be steady state (i.e. u_* must be constant with height). Equations 3, 1 and 2 above were used to calculate z/L using 1-hour average Kansas data. Equations 4 and 5 were used to calculate u_* for the layers 4-8 meters and 16-32 meters. Results are shown in Table 6.

Table 6. Comparison of Kansas u_* Values at 5.66 and 22.63 Meters

Number of Cases	Stability	$u_*(5.66 \text{ m}), \text{m/s}$	$u_*(22.63 \text{ m}), \text{m/s}$	r
20	Unstable	0.4035	0.4065	0.99
12	Stable	0.2554	0.2551	0.98
32	All	0.3479	0.3497	0.99

The values in Table 6 indicate that the Kansas data were steady state for an average data period of 1 hour. The correlation between u_* at the lower and higher levels is high. The mean values of u_* at the two levels differ by less than 1 percent.

2.4.5 Relationship of Turbulence to Wind Speed and Temperature Profile Data for 15 Minutes

The Kansas data were reduced for 15 minutes. The sampling time used to calculate σ_E and σ_A was 15 minutes. One-hour averages were obtained by averaging four successive 15-minute values.

Panofsky and Prasad⁽⁴⁾ developed a scheme for estimating σ_E from z , z_0 and L . Comparison with analysis of the Kansas data indicates that their scheme is weak for low wind speeds and high values of $\sigma_E (>7^0)$. Panofsky⁽¹⁴⁾ notes that σ_A does not obey the laws which relate wind and temperature profile data to turbulence (similarity theory). However, he suggests a statistical treatment⁽¹⁵⁾ of σ_A data which explains 37% of the variance for a particular site.

Panofsky and Prasad⁽⁴⁾ used the parameters $\ln(z/z_0)$ and $10^5 z_0/L$ to determine σ_E . Analysis of the 15-minute Kansas data described here indicates that both σ_E and σ_A at a given level are functions of z_0, L and \bar{u} . The Kansas Data were collected for 1-hour periods, each of which included four 15-minute periods. The first and last of these 15-minute periods are here used as the dependent data sample. The second and third are used as independent data. Dependent data results of least-squares fitted regression equations are seen in Table 7 for the unstable case and Table 8 for the stable case:

Table 7. Dependent Data Results for σ_E , Unstable Case

Number	Height, m	Predicted	Observed	r
		σ_E^0	σ_E^0	
36	5.65	5.5	5.5	0.89
36	11.31	5.4	5.6	0.73
36	22.63	6.03	6.03	0.93

Table 8. Dependent Data Results for σ_E , Stable Case

Number	Height, m	Predicted	Observed	r
		σ_E^0	σ_E^0	
21	5.66	4.8	4.8	0.88
21	11.31	4.1	4.1	0.90
21	22.63	3.25	3.25	0.88

Regression equations used for the 5.66 m level in the tables above are:

$$\text{Unstable case: } \sigma_E = 6.726 - 0.0402(10^5 z_0/L) - 0.2778\bar{u} \quad (11)$$

$$\text{Stable case: } \sigma_E = 6.125 - 0.0917(10^5 z_0/L) - 0.1539\bar{u} \quad (12)$$

where

σ_E is in degrees

\bar{u} is in m/s

An independent data check produced an average correlation between predicted and observed σ_E values at all three levels of 0.88 for the unstable case and 0.91 for the stable case.

Similarly, results for σ_A are seen in Tables 9 and 10. The regression equations used for the 5.66 m level in Tables 9 and 10 follow:

$$\text{Unstable case: } \sigma_A = 26.375 - 0.0796(10^5 z_0/L) - 2.26\bar{u} \quad (13)$$

$$\text{Stable case: } \sigma_A = 5.986 - 0.0359(10^5 z_0/L) + 0.2043\bar{u} \quad (14)$$

The independent data check resulted in an average correlation coefficient of 0.65 for the unstable case and 0.80 for the stable case. The maximum variation of the predicted from the observed mean was 8 percent.

Table 9. Dependent Data Results for σ_A , Unstable Case

Number	Level, m	Predicted	Observed	r
		$\bar{\sigma}_A^0$	$\bar{\sigma}_A^0$	
36	5.66	14.04	13.92	0.71
36	11.31	12.77	12.71	0.68
36	22.63	11.96	11.97	0.66

Table 10. Dependent Data Results for σ_A , Stable Case

Number	Level, m	Predicted	Observed	r
		$\bar{\sigma}_A^0$	$\bar{\sigma}_A^0$	
21	5.66	6.62	6.62	0.44
21	11.31	5.44	5.44	0.54
21	22.63	4.48	4.43	0.44

The σ_E results above are satisfactory. The σ_A results are much less so. The reason for this is apparent from inspection of the data. For successive 15-minute periods, σ_A is quite variable.

2.4.6 The Prediction of 15-Minute Turbulence Values Using Bulk Richardson's Number

If B is calculated from Equation 6, Ri from Equation 7 and z/L from Equations 1 and 2, σ_E and σ_A can be calculated from Equations 11 through 14 using $10^5 z_0/L$ derived from B and observed 5.66 m \bar{u} . The 5.66 m independent data results are seen in Table 11. The average correlation between predicted σ_E values in Table 11 is 0.92, compared to 0.90 for the results using $10^5 z_0/L$ obtained from Ri. The average r for σ_A in Table 11 is 0.72, compared to 0.71 for the results obtained using Ri. Hence, no skill is lost by substituting B for Ri and using the procedure given above to estimate Ri and $10^5 z_0/L$.

Table 11. Independent Data Prediction of 15-Minute Turbulence Values at 5.66 m Using Bulk Richardson's Number and Observed Wind Speed

Number	Stability	Predicted	Observed	Predicted	Observed	r	
		σ_{E^0}	σ_{E^0}	σ_{A^0}	σ_{A^0}		
39	Unstable	5.42	5.53	0.895	13.79	13.08	0.700
21	Stable	4.89	4.79	0.962	6.66	6.36	0.765

2.4.7 Relationship of Turbulence to Wind Speed and Temperature Profile Data for 1-Hour Average Data

Results of regression equations fitted to 1-hour average data are seen in Tables 12 through 15.

Table 12. One-Hour Average σ_E Results for the Unstable Case

Number	Level, m	Predicted σ_{E0}	Observed σ_{E0}	r
20	5.66	5.51	5.51	0.955
20	11.31	5.65	5.65	0.948
20	22.63	6.02	6.02	0.924

Table 13. One-Hour Average σ_E Results for the Stable Case

Number	Level, m	Predicted σ_{E0}	Observed σ_{E0}	r
12	5.66	4.83	4.83	0.96
12	11.31	4.06	4.06	0.966
12	22.63	3.19	3.19	0.956

Table 14. One-Hour Average σ_A Results for the Unstable Case

Number	Level, m	Predicted $\bar{\sigma}_A^0$	Observed $\bar{\sigma}_A^0$	r
20	5.66	13.54	13.54	0.86
20	11.31	12.60	12.61	0.83
20	22.63	11.78	11.78	0.81

Table 15. One-Hour Average σ_A Results for the Stable Case

Number	Level, m	Predicted $\bar{\sigma}_A^0$	Observed $\bar{\sigma}_A^0$	r
12	5.66	6.49	6.49	0.85
12	11.31	5.65	5.65	0.93
12	22.63	4.20	4.20	0.93

The 5.66 m regression equations for the above are:

$$\text{Unstable } \sigma_F = 5.741 - 0.0654(10^5 z_0/L) - 0.1454\bar{u} \quad (15)$$

$$\text{Stable } \sigma_E = 6.372 - 0.1083(10^5 z_0/L) - 0.2021\bar{u} \quad (16)$$

$$\text{Unstable } \sigma_A = 16.776 - 0.3354(10^5 z_0/L) - 1.0934\bar{u} \quad (17)$$

$$\text{Stable } \sigma_A = 5.809 - 0.0461(10^5 z_0/L) + 0.2237\bar{u} \quad (18)$$

A different basis of checking the accuracy of prediction is the standard error (S.E.) divided by the observed mean standard deviation. For the 5.66 m independent 15-minute data and for the 1-hour data, this figure is displayed in Table 16. The improvement of the 1-hour data relationship for both σ_E and σ_A prediction is marked. The unstable case σ_A prediction improves from an error of $\pm 24.1\%$ or less for 68% of the cases to 13.6%.

Table 16. Standard Error Divided by the Mean Observed Standard Deviation

	15 Minute	Independent Data	One Hour Data	
	Unstable	Stable	Unstable	Stable
Vertical S.E./ σ_E	0.054	0.0705	0.032	0.038
Horizontal S.E./ σ_A	0.241	0.0785	0.136	0.054

2.4.8 Relationship of Turbulence to the 5.66 m Mean Wind Speed and Bulk Richardson's Number for 1-Hour Average Data.

If it were possible to estimate L accurately using only wind speed and vertical temperature gradient, the basis of associating Pasquill classes with specific values of σ_E and σ_A would be assured. The assigned ΔT for each net radiation and wind speed class can be determined from Equations 9 and 10. Then the bulk Richardson number can be calculated using Equation 6. Equation 7 can be used to obtain Richardson's number from B . Equations 1 and 2 can be used to obtain z/L from Ri .

Application of the above procedure to 5.66 m 1-hour average data produced the answers in Table 17. Since no net radiometer data were available, it was necessary to use the observed 4-8 m ΔT . The regression equations used to prepare Table 17 are Equations 13 through 16. The correlation between predicted and observed turbulence values using the two methods, one based on Ri , the other on B , are almost identical.

Table 17. Predicted Values of 5.66 m σ_E and σ_A Using Bulk Richardson's Number

Number	Stability	Predicted	Observed	r	Predicted	Observed	r
		σ_E^0	σ_E^0		σ_A^0	σ_A^0	
20	Unstable	5.54	5.51	0.95	13.56	13.54	0.861
12	Stable	4.84	4.83	0.965	6.49	6.49	0.844

The maximum daytime variation of σ_E is at the higher levels. The maximum variation of σ_A is at the lower levels. Hence, it becomes important to predict the vertical gradients of σ_E and σ_A . For this purpose, the power-law relationship can be assumed for σ_E , σ_A and \bar{u} , where the respective exponents are β , α and p . Equations 4 and 5 above are the log plus linear form of the vertical wind speed profile, not the same as the power law. In spite of this, it is convenient and practical to assume a power-law form for the present treatment.

2.4.9 Calculation of β , α and p .

To determine the change of turbulence with height, the Kansas 5.66 m and 22.63 m data were used. The assumed power-law form was:

$$\frac{\sigma_E(22.63 \text{ m})}{\sigma_E(5.66 \text{ m})} = \left(\frac{22.63}{5.66} \right)^\beta \quad (19)$$

A similar form was assumed for σ_A and α as well as for \bar{u} and p . The following equations are the result of least-squares fit to the 1-hour average data:

$$\text{Unstable} \quad p = 0.1039 + 0.00157(10^5 z_0/L) + 0.00419\bar{u} \quad (20)$$

$$\alpha = -1.695p + 0.0812 \quad (21)$$

$$\beta = -5.52p + 0.674 \quad (22)$$

$$\text{Stable} \quad p = 0.3866 + 0.00737(10^5 z_0/L) - 0.0341\bar{u} \quad (23)$$

$$\alpha = -0.769p - 0.1060 \quad (24)$$

$$\beta = -1.270p - 0.0433 \quad (25)$$

where

z_0/L is for the 4-to-8-meter layer

\bar{u} is the 1-hour average wind speed at 5.66 m in m/s

The adequacy of the above equations is seen in Table 18.

If z/L used in Equations 20 through 25 is estimated from B, the results are seen in Table 19. The correlation coefficients between predicted and observed values for σ_E and σ_A at 22.63 m are all higher in Table 19 than in Table 18. Also, r is higher in Tables 18 and 19 than it is for prediction of σ_E and σ_A as functions of $10^5 z_0/L$ and \bar{u} at the 22.63 m level.

Table 18. Results of Regression Equations for p , α and β as Functions of $10^5 z_0/L$ and \bar{u}

Number	Stability	Predicted		Observed		Predicted		Observed		Predicted		Observed	
		\bar{p}	\bar{p}	$\bar{\alpha}_E$	$\bar{\alpha}_E$	$\bar{\alpha}_A$	$\bar{\alpha}_A$	$\bar{\beta}_E$	$\bar{\beta}_E$	$\bar{\beta}_A$	$\bar{\beta}_A$	$\bar{\sigma}_A$	$\bar{\sigma}_A$
20	Unstable	0.1137	0.1136	0.84	0.84	6.15	6.02	0.90	0.90	11.76	11.76	11.78	0.97
12	Stable	0.2849	0.2849	0.966	0.966	3.18	3.19	0.97	0.97	4.21	4.21	4.20	0.96

Table 19. Results of Regression Equations for p , α and β as Functions of B and \bar{u}

Number	Stability	Predicted		Observed		Predicted		Observed		Predicted		Observed	
		\bar{p}	\bar{p}	$\bar{\alpha}_E$	$\bar{\alpha}_E$	$\bar{\alpha}_A$	$\bar{\alpha}_A$	$\bar{\beta}_E$	$\bar{\beta}_E$	$\bar{\beta}_A$	$\bar{\beta}_A$	$\bar{\sigma}_A$	$\bar{\sigma}_A$
20	Unstable	0.1133	0.1136	0.84	0.84	6.00	6.02	0.97	0.97	11.69	11.69	11.78	0.977
12	Stable	0.2843	0.2849	0.963	0.963	3.17	3.19	0.974	0.974	4.18	4.18	4.20	0.972

These results appear in Tables 12 through 15. The overall average 22.63 m r in Tables 12-15 is 0.905, compared to 0.973 for σ_E and σ_A in Table 19. Part of the reason for this may be the relatively small range of the ΔT values for the 16 to 32 m layer and hence the relatively insensitive values of $10^5 z_0/L$.

2.4.10 Tabulation of Kansas Values for $1/L$, L , p , α , β , σ_E and σ_A in Pasquill-Turner Tables.

From Table 3 and Equation 10, values for $\partial\theta/\partial z$ can be assigned for every wind speed and radiative index category. The radiative index categories are 4, 3, 2, 1, 0, -1 and -2. For the 0 category, $\partial\theta/\partial z$ is assumed to equal zero. B is then calculated using Equation 6. Ri is calculated from B , using Equation 7. z/L is calculated from Equations 1 and 2. Tabulated values of $1/L$ and L are seen in Table 20. The $\partial\theta/\partial z$ stable limit values for radiation indexes 4 through 1 are -0.115, -0.101, -0.07 and -0.035, respectively. The stable limit values used for indexes -1 and -2 appear in Table 4 above.

Using the values of L in Table 20 and a roughness of 0.0244 m, the σ_E and σ_A values in Table 21 were calculated from Equations 15 through 18. The range of 1-hour-average wind speeds observed for the unstable classes (4-1) was 4-8 m/s. The range for the stable classes was 2.45 to 6.4 m/s; hence the accuracy of the σ_E and σ_A estimates outside of this range is not known.

The p , α and β values for \bar{u} , σ_E and σ_A profiles can be obtained from Equations 20 through 25. Results appear in Table 22. From the p , α , and β values in Table 22, the 22.63 m values of \bar{u} , σ_E and σ_A can be calculated from the power-law equation (Equation 19). Results for σ_E and σ_A appear in Table 23.

The average observed ratio of σ_A/σ_E for the unstable 5.66 m case was 2.45. The average stable case ratio was 1.34. At 22.63 m, the average unstable case ratio was 1.96, and the stable case ratio was 1.31. The variation of these ratios with 5.66 m wind speed and radiation index can be seen in Tables 21 and 23.

Table 20. Values of L and 1/L by Wind Speed and Radiation Index Class

5.66 m \bar{u} , m/s	Net Radiation Index											
	4		3		2		1		0		-1	
	1/L	L, m	1/L	L, m	1/L	L, m	1/L	L, m	1/L	L, m	1/L	L, m
2	-0.59	-1.7	-0.51	-2.0	-0.33	-3.1	-0.13	-7.5	0	∞	0.11	9.0
3	-0.22	-4.6	-0.18	-5.4	-0.11	-8.8	-0.045	-22.1	0	∞	0.05	20.0
4	-0.10	-9.8	-0.08	-11.9	-0.05	-18.9	-0.022	-46.2	0	∞	0.026	39.0
5	-0.06	-17.7	-0.05	-21.1	-0.03	-33.1	-0.010	-96.0	0	∞	0.017	59.0
6	-0.035	-28.6	-0.03	-33.1	-0.02	-53.4	-0.008	-121.5	0	∞	0.006	167.0
7	-0.024	-42.3	-0.02	-49.8	-0.013	-77.7	-0.006	-170.7	0	∞	0.0015	653.0
8	-0.017	-58.8	-0.015	-68.6	-0.010	-103.2	-0.0045	-222.0	0	∞	0	∞
9	-0.013	-78.4	-0.011	-90.7	-0.007	-139.2	-0.004	-283.0	0	∞	0	∞

Table 21. Expected 5.66 m σ_E and σ_A Values for Each Radiation Index and Wind Speed

5.66 m \bar{u} , m/s	Net Radiation Index											
	3			2			1			0		
	σ_E^0	σ_A^0	σ_E^0	σ_A^0	σ_E^0	σ_A^0	σ_E^0	σ_A^0	σ_E^0	σ_A^0	σ_E^0	σ_A^0
2	15.0	50.0	13.7	45.0	10.7	35.0	7.6	22.3	5.5	14.6	3.1	5.0
3	9.0	31.0	8.3	28.6	7.0	22.8	6.0	17.0	5.3	13.5	4.5	5.9
4	7.0	21.0	6.5	19.3	6.0	16.7	5.5	14.0	5.2	12.4	4.9	6.4
5	6.0	16.0	5.8	15.0	5.5	13.8	5.2	12.0	5.0	11.3	4.9	6.7
6	5.4	13.0	5.4	12.7	5.2	11.7	5.0	10.9	4.9	10.2	5.0	7.1
7	5.1	11.0	5.0	10.8	4.9	10.2	4.8	9.6	4.7	9.1	4.9	7.4
8	4.9	9.4	4.8	9.2	4.7	8.8	4.7	8.4	4.6	8.0	4.7	7.6
9	4.6	8.0	4.6	7.8	4.5	7.5	4.5	7.2	4.4	7.2	4.5	7.2

Table 22. Power Law Exponents for 5.66 to 22.63 m Values of \bar{u} , σ_A , and σ_E

5.66 m 3m/s	Net Radiation Index																					
	4		3		2		1		0		-1		-2									
	P	a	P	a	P	a	P	a	P	a	P	a	P	a	P	a	P	a	P	a	P	a
2							0.06	-0.016	0.36	0.29	-0.26	-0.12	0.51	-0.50	-0.81	0.57	-0.54	-0.68				
3	0.02	0.04	0.55	0.04	0.01	0.45	0.07	-0.04	0.29	0.10	-0.09	0.13	0.24	-0.24	-0.15	0.37	-0.39	-0.43	0.40	-0.41	-0.47	
4	0.08	-0.06	0.24	0.09	-0.06	0.20	0.10	-0.09	0.12	0.11	-0.11	0.05	0.70	-0.22	-0.14	0.30	-0.33	-0.33	0.32	-0.35	-0.36	
5	0.10	-0.09	0.11	0.11	-0.10	0.09	0.11	-0.11	0.05	0.12	-0.12	0.01	0.18	-0.21	-0.13	0.25	-0.30	-0.27	0.25	-0.30	-0.28	
6	0.115	-0.11	0.04	0.12	-0.12	0.25	0.12	-0.125	0	0.126	-0.13	-0.02	0.16	-0.19	-0.11	0.19	-0.25	-0.20	0.20	-0.26	-0.22	
7	0.124	-0.13	-0.01	0.125	-0.13	-0.02	0.13	-0.136	-0.03	0.13	-0.14	-0.05	0.14	-0.18	-0.10	0.15	-0.22	-0.15	0.16	-0.23	-0.16	
8	0.13	-0.14	-0.05	0.132	-0.14	-0.05	0.134	-0.145	-0.06	0.136	-0.15	-0.06	0.12	-0.17	-0.09	0.11	-0.19	-0.10	0.12	-0.20	-0.11	
9	0.137	-0.15	-0.06	0.137	-0.15	-0.06	0.139	-0.154	-0.09	0.14	-0.16	-0.10	0.11	-0.163	-0.08	0.08	-0.17	-0.06	0.08	-0.17	-0.06	

Table 23. Expected 22.63 m σ_E and σ_A Values for 5.66 m Net Radiation Index and Wind Speed

		Net Radiation Index											
5.66 m		3				2				1			
$u, \text{ m/s}$		σ_E^0	σ_A^0	σ_E^0	σ_A^0	σ_E^0	σ_A^0	σ_E^0	σ_A^0	σ_E^0	σ_A^0	σ_E^0	σ_A^0
2													
3	19.0	33.0	15.5	29.0	10.5	21.6	12.5	21.8	4.7	10.2	1.3	2.5	1.2
4	10.0	20.0	8.6	17.8	7.1	14.7	7.2	15.0	4.3	9.7	2.5	3.4	2.1
5	8.0	14.0	6.6	13.1	5.9	11.8	5.9	12.0	4.3	9.1	3.1	4.0	2.8
6	6.0	11.0	5.6	10.8	5.2	9.8	5.3	10.2	4.2	8.4	3.4	4.5	3.3
7	5.0	9.2	4.9	9.0	4.7	8.4	4.9	9.1	4.2	7.8	3.8	5.4	3.5
8	4.6	7.7	4.5	7.6	4.3	7.2	4.5	7.9	4.1	7.1	4.0	5.5	3.8
9	4.1	6.5	4.1	6.3	4.0	6.0	4.2	6.8	4.1	6.3	4.1	5.8	4.0
							3.9	5.8	3.9	5.7	3.9	5.8	3.9
													5.8

2.4.11 Similarity Theory Methods of Calculating σ_E and σ_A .

Businger⁽¹²⁾ documents a universal law for determining vertical turbulence in the unstable case:

$$\sigma_w/u_* = 2 (-z/L)^{1/3} \quad (26)$$

where

σ_w = standard deviation of vertical velocity in m/s

Since the $1/L$ values are shown in Table 20 and u_* can be calculated from Equation 4, it is a simple matter to estimate σ_w for each $1/L$ value at 5.66 m. Then σ_E is obtain from:

$$\sigma_E = 57.3 \sigma_w / \bar{u} \text{ degrees} \quad (27)$$

where

\bar{u} = 5.66 m wind speed in m/s

Equation 26 applies for $-z/L \geq 0.3$ ⁽¹²⁾. For $-z/L < 0.3$, the ratio becomes constant:

$$\sigma_w/u_* = 1.34 \quad (28)$$

The correlation of the 32 unstable case σ_E values in Table 21 with σ_E calculated from Equations 26 through 28 resulted in a coefficient of 0.99.

In an effort to represent the standard deviation of lateral velocity variation (σ_v), the 20 one-hour values of $\ln(\sigma_v/u_*)$ were least-squares fitted to $\ln(-z/L)$. The resulting formula is:

$$\sigma_v/u_* = 4.67(-z/L)^{1/3.25} \quad (29)$$

Kansas data show this formula to be applicable for $-z/L > 0.066$. For smaller values, $\sigma_v/u_* = 2$. For 20 one-hour average values, the correlation of the predicted σ_v/u_* with the observed values was 0.74. This is not too good, but the formula is useful as a basis of estimating σ_A for the unstable, low-wind speed cases. The Equation 29 values were averaged with the regression equation values to supply the figures appearing in the 2m/s unstable index cases (4-1) in Table 21.

2.4.12 Comparison of Unstable Case Similarity Theory Estimates of σ_E to Panofsky Prasad and Regression Equation Estimates.

Values for σ_E obtained from regression Equation 15 (Reg), Equations 26 and 27 (Sim) can be compared to values obtained from the Panofsky and Prasad⁽⁴⁾ graph (P). Results appear in Table 24.

Table 24. Comparison of 5.66 m σ_E Values Obtained by Three Methods

5.66 m \bar{u} , m/s	4			Net Radiation Index						1			Average		
	Reg	Sim	P	Reg	Sim	P	Reg	Sim	P	Reg	Sim	P	Reg	Sim	P
2	15.0	16.8[9.0]		13.7	15.4	[7.0]	10.7	12.3	6.3	7.6	8.2	5.8	11.8	13.2	7.0
3	9.0	10.2	6.0	8.3	9.5	5.9	7.0	7.6	5.7	6.0	5.4	5.6	7.6	8.2	5.8
4	7.0	7.3	5.8	6.5	6.8	5.6	6.0	5.5	5.6	5.5	5.2	5.5	6.2	6.2	5.6
5	6.0	5.7	5.6	5.8	5.5	5.5	5.5	5.3	5.5	5.2	5.1	5.5	5.6	5.4	5.5

The regression equation results and similarity theory results in Table 24 are quite close. The Panofsky and Prasad figure produces σ_E values too low for wind speeds of 2 and 3 m/s. The Panofsky and Prasad figure for σ_E could be improved if values of $-10^5(z_0/L)$ greater than 100 were considered. The bracketed figures in Table 24 required extrapolations of the Panofsky figure, since the $-10^5(z_0/L)$ values were greater than 100.

2.4.13 The Calculated Turbulence Values for the 10-Meter Level.

It is standard practice to use the 10 m \bar{u} to determine the Pasquill stability category. The turbulence values applicable at 10 meters appear in Table 25.

The results of Table 2 can now be used to assign Pasquill stability class values to σ_E and σ_A as shown in Table 25. The result appears in Table 26. It is notable in Table 26 that in 15 cases (25%), the Pasquill classes for σ_E and σ_A are different. Also, the usual neutral-case class D does not appear at all in the 0 radiation index class. This suggests the site dependence of a given Pasquill category as well as the dependence on radiation class, wind speed and surface roughness.

Table 25. Expected 10 m σ_E and σ_A values for 10 m Wind Speed and 5.66 Net Radiation Index

10 m \bar{u} m/s	Net Radiation Index											
	4	3	2	1	0	-1	-2					
	σ_A^0	σ_E^0	σ_A^0	σ_E^0	σ_A^0	σ_E^0	σ_A^0	σ_E^0	σ_A^0	σ_E^0	σ_A^0	σ_E^0
2												
3	19.5	33.8	16.4	30.4	11.3	23.2	9.0	17.3	4.7	10.2	1.3	2.5
4	13.0	24.4	11.3	22.2	8.7	17.8	6.6	13.6	4.4	9.8	1.3	2.5
5	9.2	17.5	7.9	16.1	6.7	13.7	5.7	11.5	4.3	9.3	2.5	3.4
6	7.6	13.4	6.5	12.8	5.8	11.5	5.3	10.1	4.2	8.7	3.1	4.0
7	6.1	11.1	5.7	10.9	5.2	9.9	4.9	9.2	4.2	8.1	3.4	4.5
8	5.2	9.6	5.1	9.5	4.9	8.8	4.6	8.3	4.2	7.5	3.8	5.4
9	4.8	8.4	4.7	8.3	4.5	7.8	4.4	7.4	4.1	6.7	4.0	5.7
10	4.4	7.3	4.4	7.2	4.2	6.9	4.1	6.5	4.0	6.0	3.9	5.8

^aBracketed values are arbitrary estimates.

Table 26. Pasquill Stability Class for Kansas Data

10 m \bar{u} m/s	Net Radiation Index													
	4		3		2		1		0		-1		-2	
	σ_E	σ_A	σ_E	σ_A	σ_E	σ_A	σ_E	σ_A	σ_E	σ_A	σ_E	σ_A	σ_E	σ_A
2							A	A	C	B	F	F	F	F
3	A	A	A	A	A	A	A	A	C	B	F	F	F	F
4	A	A	A	A	A	A	B	A	C	B	F	F	F	F
5	A	A	A	A	B	A	B	B	C	B	D	E	E	E
6	A	A	B	B	B	B	B	B	C	C	D	D	D	E
7	B	B	B	B	B	B	C	B	C	C	C	D	D	D
8	B	B	C	B	C	C	C	C	C	C	C	D	C	D
9	C	C	C	C	C	C	C	C	C	C	C	D	C	D
10	C	C	C	C	C	C	C	C	C	C	C	C	C	C

2.4.14 Calculation of Surface Roughness.

Surface roughness can be estimated for the neutral case ($\partial\theta/\partial z = 0$) from the equation:

$$\begin{aligned}\bar{u}(z) &= \frac{u_*}{k} (\ln(z/z_0)) \\ &= \frac{u_*}{k} (\ln z - \ln z_0)\end{aligned}\quad (31)$$

For an example of the application of Equation 31, see the Wangara report.⁽⁶⁾ Each wind speed profile is treated independently by first plotting the profile on $\ln z$ versus \bar{u} coordinate paper. Then the data is least-squares fitted up to the highest level wind speed which falls on an eye-fitted straight line. Since u_* is constant with height, it is possible to solve for z_0 .

A similar technique can be applied to the unstable case data using Equation 4. This technique was used⁽¹²⁾ to determine roughness for the Kansas data.

2.5 ANALYSIS

The results above indicate that the bulk Richardson number is a powerful tool to estimate turbulence at a particular site. At a given height, this number can be calculated using vertical temperature gradient and wind speed only. The agreement of regression-equation estimates of σ_E with the estimates prepared from a universal equation (Equation 26) is reassuring, although applicable only to unstable case data. Table 26 indicates that the Pasquill stability classes for vertical and horizontal diffusion cloud growth are frequently not the same (25% of the time). The expected prediction accuracy for 90% of the cases is $\pm 27.2\%$ for unstable case 1-hour average σ_A estimates and $\pm 6\%$ for the unstable case σ_E . Using the observed median of σ_A Pasquill class A as the reference, the prediction error might be $\pm 4^\circ$ for 90% of the cases or $\pm 2^\circ$ for 68% of the cases. This compares to an observed class range of 8° . In the case of σ_E , the predicted unstable case error is $\pm 6.4\%$ for 90% of the cases. This means an error of $\pm 0.6^\circ$ for class A compared to a class A observed range of 5° , $\pm 0.4^\circ$ for class B versus a class range of 1.85° and $\pm 0.25^\circ$ for class C versus a class range of 1.85° . This suggests that 1-hour average values of σ_A can be predicted accurately within plus or minus one class and that σ_E values can be predicted with much greater precision. Prediction of stable case σ_E values is almost as good as the unstable case results above, whereas prediction of σ_A improves from 27.2 to $\pm 10.8\%$ for 90% of the cases.

2.6 CONCLUSION

The above results show that a simple measurement of vertical temperature gradient and \bar{u} can be used to accurately predict vertical or horizontal turbulence for any combination of radiation index and wind speed. It remains to be seen whether measured net radiation can adequately substitute for vertical temperature gradient. The empirical equations required to implement the technique require collection of data at a fully instrumented tower. Observations of cloud cover and net radiation would

make it possible to compare results to those obtained from the Pasquill and Turner bases of classification as well as to determine whether measured net radiation is a more satisfactory indicator of net radiation index and, hence, of vertical temperature gradient.

REFERENCES

1. Gifford, F.A., "Use of Routine Meteorological Observations for Estimating Atmospheric Dispersion," Nuclear Safety, Vol 2, No.4, p.47-51, 1961.
2. U.S. Department of Health, Education and Welfare, Cincinnati, Ohio, Workbook of Atmospheric Dispersion Estimates (U), by D. Bruce Turner, 1969.
3. U.S. Nuclear Regulatory Commission, Washington D.C., Regulatory Guide 1.23: Onsite Meteorological Programs. Safety Guides for Water Cooled Nuclear Power Plants, p. 23.1 - 23.13, 1972.
4. Panofsky, H.A., and B. Prasad, "Similarity Theories and Diffusion," Int. J. Air Wat. Poll., Vol 9. p. 419-430, 1965.
5. Lettau, H.H., and Ben Davidson, Exploring the Atmosphere's First Mile, Vol. II, Pergamon Press, 1957.
6. Commonwealth Scientific and Industrial Research Organization, Australia, The Mangara Experiment: Boundary Layer Data, by R.H. Clarke, et al., 1971
7. Air Force Cambridge Research Laboratories, Bedford, Mass., Kansas 1968 Field Program Data Report, Yutaka Izumi, Editor, 1971.
8. Golder, D.G., "A Comparison of Stability Parameters," Pennsylvania State U., Masters Thesis, December 1970.
9. Luna, R.E., and H.W. Church, "A Comparison of Turbulence Intensity and Stability Ratio Measurements to Pasquill Stability Classes," J. Appl. Meteor. Vol 11, p. 663-669, 1972.
10. Gifford, F.A., "Turbulent Diffusion-Typing Schemes: A Review," Nuclear Safety, Vol 17, No.1, p. 68-86, 1976.
11. Prasad, B., "Wind and Temperature Fluctuations in the Surface Layer." Doctoral Thesis, Department of Meteorology, Pennsylvania State Univ., 1967.
12. Businger, Joost A., "Turbulent Transfer in the Atmospheric Surface Layer," Workshop on Micrometeorology, American Meteorological Society, p. 67-100, 1973.
13. Turner, Bruce D., "A Diffusion Model for an Urban Area," Journal of Applied Meteorology, Volume 3, p. 83-91, 1964.

14. Panofsky, Hans A., "Tower Micrometeorology," Workshop on Micrometeorology American Meteorological Society, p. 151-176, 1973.

15. Panofsky, H.A. and L. Kristensen, "Climatology of Wind Direction Fluctuations at Riso," Journal of Applied Meteorology, Volume 15, p.1279-1283, 1976.

DISTRIBUTION LIST

	<u>Copies</u>
Director National Oceanic & Atmospheric Administration Environmental Research Laboratories Boulder, CO 80302	1
Director National Oceanic and Atmospheric Administration 8060 13th Street Silver Spring, MD 20910	1
Director, National Oceanic & Atmospheric Administration Technical Processes Branch, D823 Room 806, Libraries Division 8060 13th Street Silver Spring, MD 20910	1
Director National Oceanic & Atmospheric Administration National Oceanographic Data Center, D722 Rockville, MD 20852	1
NASA Scientific and Technical Information Facility ATTN: Acquisitions Branch (S-AK/DL) P. O. Box 33 College Park, MD 20740	1
Environmental Protection Agency Division of Meteorology Research Triangle Park, NC 27711	2
National Aeronautics and Space Administration Director of Meteorological Systems Office of Applications (FM) Washington, DC 20546	1
Chief Environmental Data Service Atmospheric Sciences Library Grammax Building ATTN: D821 Silver Spring, MD 20910	1
Commander U.S. Army White Sands Missile Range ATTN: STEWS-TE-ER Technical Library White Sands Missile Range, NM 88002	1

	<u>Copies</u>
Commander ECOM Atmospheric Sciences Laboratory White Sands Missile Range, NM 88002	3
Commander U.S. Army Foreign Science and Tech Center 220 Seventh Street, NE Charlottesville, VA 22901	1
Assistant Secretary of the Navy (R&D) Department of the Navy ATTN: Special Assistant (Research) Washington, DC 20350	1
Director Atmospheric Physics & Chem Lab Code 31, NOAA Department of Commerce Boulder, CO 80302	2
Rome Air Development Center ATTN: Documents Library TILD (Bette Smith) Griffiss Air Force Base, NY 13441	1
Air Force Cambridge Rsch Labs ATTN: LCH (A. S. Carten, Jr.) Hanscom AFB Bedford, MA 01731	3
Director Defense Nuclear Agency ATTN: Tech Library Washington, DC 20305	4
Head, Atmospheric Research Section National Science Foundation 1800 G. Street. NW Washington, DC 20550	1
Commander U.S. Army Electronics Command ATTN: DRSEL-CT-S (Dr. Swingle) Fort Monmouth, NJ 07703	1
Meteorology Laboratory AFCRL/LY Hanscom AFB Bedford, MA 01731	2

	<u>Copies</u>
National Weather Service National Meteorological Center World Weather Bldg - 5200 Auth Rd ATTN: Mr. Quiroz Washington, DC 20233	1
National Center for Atmos Res NCAR Library PO Box 3000 Boulder, CO 80303	1
Head, Rsch and Development Div (ESA-131) Meteorological Department Naval Weapons Engineering Support Act Washington, DC 20374	1
HQDA (DAEN-RDM/Dr. De Percin) Forrestal Bldg Washington, DC 20314	2
The Library of Congress ATTN: Exchange & Gift Div Washington, DC 20540	2
NOAA Weather Service Nuclear Spt Ofc ATTN: Mr. R. W. Titus PO Box 14985 Las Vegas, NV 89114	1
SAMTEC - WE ATTN: Mr. R. W. Lenhard Vandenberg AFB, CA 93437	1
Department of Atmospheric Science University of Washington Seattle, WA 98195	1
Commander U.S. Air Force Environmental Technical Applications Center Scott Air Force Base, IL 62225	1
RACIC, Battelle Memorial Institute Columbus Laboratories 505 King Avenue Columbus, OH 43201	1

	<u>Copies</u>
Director Western Regional Headquarters National Weather Service P.O. Box 11188, Federal Building Salt Lake City, UT 84111	1
Director U.S. Army Engineer Waterways Experiment Station ATTN: WES-FV Vicksburg, MS 39181	1
Director National Sciences Foundation Atmospheric Sciences Programs Washington, DC 20550	1
Director Federal Aviation Agency Bureau of Research and Development Washington, DC 20553	1
U.S. Department of Agriculture Forest Service Pacific Southwest Forest and Land Experiment Station ATTN: Mr. Jerry R. Reid 1960 Addison Street, P.O. Box 245 Berkeley, CA 94701	1
The Research Corporation of New England ATTN: Mr. Donald L. Shearer 125 Silas Deane Highway Wethersfield, CT 06109	1
Battelle Northwest Laboratories ATTN: Dr. Larry L. Wendell Bldg 622R, 200 West Area Richland, WA 99352	1
Administrator Defense Documentation Center Camden Station Alexandria, VA 22314	2
H. B. Cramer Co, Inc P.O. Box 8049 Salt Lake City, Utah 84108	1

Director, Meteorology Department
Pennsylvania State University
University Station, PA 16802

Copies

1

Meteorology Department
University of Utah
Salt Lake City, UT 84116

1

Commander
U.S. Army Dugway Proving Ground
Dugway, UT 84022

30

Distribute as follows:

STEDP-SC	(1)
MT-S	(25)
MT-S-L	(1)
MT-T-M	(1)
MT-DA	(2)